

1 **Transcribed germline-limited coding sequences in *Oxytricha trifallax***

2 **Richard V. Miller^{1,2}, Rafik Neme^{1,3}, Derek M. Clay^{1,2}, Jananan S. Pathmanathan^{1,4},**

3 **Michael W. Lu^{1,6}, V. Talya Yerlici^{1,5}, Jaspreet S. Khurana^{1,6}, and Laura F. Landweber^{1,6,*}**

4 **¹ Department of Biochemistry and Molecular Biophysics, Columbia University, New York,**
5 **NY 10032, USA**

6 **² Department of Molecular Biology, Princeton University, Princeton, NJ 08544, USA**

7 **³ Current address: Department of Chemistry and Biology, Universidad del Norte,**
8 **Barranquilla, Colombia**

9 **⁴ Current address: School of Environmental and Biological Sciences, Rutgers University,**
10 **New Brunswick, NJ 08901, USA**

11 **⁵ Current address: Department of Laboratory Medicine and Pathobiology, Faculty of**
12 **Medicine, University of Toronto, Toronto, ON M5G 1M1, Canada**

13 **⁶ Current address: Strand Therapeutics, Cambridge, MA 02139, USA**

14 **⁶ Department of Biological Sciences, Columbia University, New York, NY 10027, USA**

15

16 Running Head: *Oxytricha* transcribed germline-limited ORFs

17 Keywords: germline; genome rearrangement; DNA elimination; noncoding RNA; ciliate;

18 micronucleus

19 *To whom correspondence should be addressed:

20 **Laura F. Landweber**

21 Department of Biochemistry and Molecular Biophysics, Columbia University, New York, NY

22 10032, USA

23 Phone: +1 212 305-3898

24 Email: Laura.Landweber@columbia.edu

25

26 **Abstract**

27 **The germline-soma divide is a fundamental distinction in developmental biology,**
28 **and different genes are expressed in germline and somatic cells throughout metazoan life**
29 **cycles. Ciliates, a group of microbial eukaryotes, exhibit germline-somatic nuclear**
30 **dimorphism within a single cell with two different genomes. The ciliate *Oxytricha trifallax***
31 **undergoes massive RNA-guided DNA elimination and genome rearrangement to produce a**
32 **new somatic macronucleus (MAC) from a copy of the germline micronucleus (MIC). This**
33 **process eliminates noncoding DNA sequences that interrupt genes and also deletes**
34 **hundreds of germline-limited open reading frames (ORFs) that are transcribed during**
35 **genome rearrangement. Here, we update the set of transcribed germline-limited ORFs**
36 **(TGLOs) in *O. trifallax*. We show that TGLOs tend to be expressed during nuclear**
37 **development and then are absent from the somatic MAC. We also demonstrate that**
38 **exposure to synthetic RNA can reprogram TGLO retention in the somatic MAC and that**
39 **TGLO retention leads to transcription outside the normal developmental program. These**
40 **data suggest that TGLOs represent a group of developmentally regulated protein coding**
41 **sequences whose gene expression is terminated by DNA elimination.**

42

43 **Introduction**

44 Ciliates are a lineage of microbial eukaryotes characterized by functional nuclear
45 differentiation. Each ciliate cell has one or more somatic macronuclei (MAC) and one or more
46 germline micronuclei (MIC). The somatic MAC contains the somatic genome, consisting of over
47 17,000 gene-sized nanochromosomes that are transcribed throughout the organism's life cycles
48 (Swart et al. 2013; Lindblad et al. 2019). The germline genome is a fragmented and scrambled
49 version of the somatic genome that undergoes a complex process of DNA deletion and
50 rearrangement during sexual reproduction (Chen et al. 2014).

51 Previous studies have shown that *Oxytricha*'s sexual rearrangement cycle is guided by
52 several noncoding RNA pathways. In the early stages of the sexual life cycle, bidirectional
53 transcription across the length of nanochromosomes produce thousands of long template RNAs
54 from the parental MAC (Lindblad et al. 2017). These transcripts guide the rearrangement of
55 macronuclear destined sequences (MDSs) during development, and previous experiments
56 showed that injection of synthetic template RNAs could program aberrant rearrangements
57 (Nowacki et al. 2008; Bracht et al. 2017; Nowacki et al. 2011). Millions of 27-nucleotide long
58 PIWI-associated small RNAs (piRNAs) are abundant during early *Oxytricha* rearrangement and
59 interact with the *Oxytricha* PIWI ortholog Otiwi-1. These piRNAs also derive from the parental
60 MAC. Their role is to protect the sequences they target against DNA deletion during
61 development of the zygotic MAC. Injection of synthetic piRNA sequences that target internal
62 eliminated sequences (IESs) that interrupt MDSs in the MIC can prevent their deletion during
63 rearrangement and program their retention in the MAC (Fang et al. 2012). Programmed IES
64 retention is now used as a genetic tool to create somatic knockout strains in *Oxytricha* (Khurana
65 et al. 2018; Beh et al. 2019).

66 Besides IESs and transposons that are eliminated during development, *Oxytricha* has
67 other classes of germline-specific MIC DNA sequences (Chen et al. 2016). Analysis of the
68 germline MIC genome together with transcriptome-guided gene prediction previously uncovered
69 810 germline-limited protein coding genes encoded in the MIC genome (Chen et al. 2014).
70 These germline-limited genes are specifically transcribed during rearrangement, and 26% of
71 them had demonstrated translation of peptides present in a survey of one developmental time
72 point.

73 Other lineages also have germline-limited protein coding sequences, including the ciliate
74 *Tetrahymena thermophila* (Hamilton et al. 2016; Lin et al. 2016; Feng et al. 2017), the parasitic
75 roundworm *Ascaris suum* (Wang et al. 2012; Wang et al. 2017), and the sea lamprey *Petromyzon*
76 *marinus* (Bryant et al. 2016; Smith et al. 2009; Smith et al. 2012; Timoshevskiy et al. 2016;
77 Timoshevskiy et al. 2017). Protein coding sequences are discarded in all these cases, and genes
78 eliminated from somatic lineage cells are typically predicted to have functions in the germline
79 and embryogenesis (Smith et al. 2012; Bryant et al. 2016). The songbird *Taeniopygia guttata* has
80 a germline-limited chromosome that is deleted from somatic lineage cells (Pigozzi and Solari
81 1998; Pigozzi and Solari 2005; Itoh et al. 2009; Biederman et al. 2018; Kinsella et al. 2019;
82 Torgasheva et al. 2019).

83 Here, we update and expand the set of transcribed germline-limited ORFs (TGLOs) in
84 *Oxytricha* and provide functional experiments that reprogram the somatic retention of a small
85 number of TGLOs to test the hypothesis that developmental deletion is the main mechanism to
86 repress their gene expression during asexual growth. Like the previous set of germline-limited
87 genes, we show that TGLOs contain several predicted functions and conserved domains that
88 could be involved in *Oxytricha* development. This work also identified a locus, g11288, that is

89 retained in the somatic MAC of a subset of progeny cells, revealing an example of a strain-
90 specific macronuclear chromosome.

91 **Materials and methods**

92 **Illumina library preparation and sequencing**

93 Genomic DNA was collected from mated *O. trifallax* cells at various developmental
94 time-points using the Nucleospin genomic DNA spin column column (Machery-Nagle). Illumina
95 DNA sequencing libraries were prepared using the NEBNext Ultra II library preparation kit
96 (New England Biolabs). 2 x 250 bp paired end sequencing reads were obtained using an Illumina
97 HiSeq 2500, and remaining adapter sequences were trimmed using Trim Galore! software in the
98 Galaxy cloud computing environment.

99 Total RNA was extracted from mated *O. trifallax* cells at various developmental time-
100 points using Trizol reagent (Thermo Fisher, Waltham, MA, USA). Contaminating DNA was
101 removed using a Turbo DNase kit (Thermo Fisher, Waltham, MA, USA). Poly-adenylated
102 transcripts were enriched using the NEBNext Poly(A) mRNA Magnetic Isolation Module (New
103 England Biolabs, Ipswich, MA, USA). RNA sequencing libraries were prepared using the
104 ScriptSeq version 2 kit (Illumina, San Diego, CA, USA). 2 x 75 bp paired end sequencing reads
105 were obtained using an Illumina HiSeq 2500, and remaining adapter sequences were trimmed
106 using Trim Galore! software in the Galaxy cloud computing environment.

107 **TGLO computational prediction**

108 We predicted TGLOs using a previously published pipeline for germline-limited gene
109 prediction with some modifications (Chen et al. 2014). We predicted coding sequences with
110 AUGUSTUS (version 3.3.0) (Stanke et al. 2006) using a gene prediction model trained on *O.*
111 *trifallax* somatic MAC genes and transcripts as hints. We generated hint files for the gene
112 prediction software by mapping RNA-seq data from cells collected at various time points to the
113 germline MIC genome using HISAT2 (version 2.0.5). We ran AUGUSTUS with the options --

114 UTR=on and --alternatives-from-evidence=true. We filtered AUGUSTUS gene predictions to
115 keep only models supported by hints including at least four supporting RNA-seq reads and
116 greater than 80% of the coding sequence covered by RNA-seq reads to obtain the high
117 transcription dataset. We kept only models supported by hints including at least two supporting
118 RNA-seq reads and required greater than 20% of the coding sequence be covered by RNA-seq
119 reads to obtain the low transcription dataset. We also removed candidate sequences with more
120 than a minimal number of whole cell genomic DNA reads mapped from asexually growing
121 cultures of either parental genotype or a pool of F1 cells to ensure that MAC encoded candidates
122 were removed while accounting for the fact that some MIC encoded sequences will be present in
123 whole cell sequencing reads.

124 **DNA sequencing analysis**

125 Genomic DNA sequencing reads were aligned to the *O. trifallax* MIC genome assembly
126 using BWA-MEM (version 0.7.17) with the -M option to mark short split alignments as
127 supplementary alignments. Alignment files were processed using the Samtools software package
128 (version 0.1.20) (Li et al. 2009). FeatureCounts software (version 2.0.0) (Liao et al. 2014) was
129 used to assess the raw number of reads mapping to *O. trifallax* genome features (Burns et al.
130 2016). Relative DNA copy number changes for each genome feature were normalized using the
131 R/Bioconductor package DESeq2 (version 1.26.0) (Love et al. 2014). Heat maps showing
132 normalized DNA copy number during the developmental life cycle were generated using the
133 log₂ normalized copy number values and the pheatmap R package (version 1.0.12).

134 **Transcriptome sequencing analysis**

135 Poly(A)-selected RNA sequencing reads were aligned to the *O. trifallax* MAC genome
136 assembly and MIC genome assembly using HISAT2 (version 2.0.4) and Bowtie2 in the local

137 alignment mode, respectively. Relative DNA copy number changes were normalized using the
138 R/Bioconductor package DESeq2. Alignment files were processed using the Samtools software
139 package (version 0.1.20) (Li et al. 2009). FeatureCounts software (version 2.0.0) (Liao et al.
140 2014) was used to assess the raw number of reads mapping to *O. trifallax* genome features
141 (Burns et al. 2016). Relative RNA expression changes for each genome feature were normalized
142 using the R/Bioconductor package DESeq2 (version 1.26.0) (Love et al. 2014). Heat maps
143 showing normalized RNA expression during the developmental life cycle were generated using
144 the log₂ normalized copy number values and the pheatmap R package (version 1.0.12). Two
145 timepoints of triplicate RNA-seq reads (12 hr and 36 hr) from the late time-course were
146 previously uploaded to the European Nucleotide Archive under the project number
147 PRJEB32087.

148 **Small RNA sequencing analysis**

149 Previously sequenced Otiwi-1-dependent piRNAs (Fang et al. 2012) were aligned to the
150 *O. trifallax* MIC genome assembly using Bowtie2 (version 2.3.4.1) in the local alignment mode.
151 Alignment files were processed using the Samtools software package (version 0.1.20) (Li et al.
152 2009), and alignments were viewed in the context of the MIC genome using the Integrative
153 Genomics Viewer (version 2.7.2) (Robinson et al. 2011).

154 **Mass spectrometry analysis**

155 Raw data were analyzed using MaxQuant (version 1.6.3.4) to search against a combined
156 database containing previously published macronuclear-encoded and MIC-limited genes in
157 addition to either highly-transcribed or lowly-transcribed TGLOs (Chen et al. 2014). Searches
158 were performed using Trypsin/P as the enzyme with a maximum of two missed cleavages,
159 methionine oxidation and protein N-terminal acetylation as variable modifications, cysteine

160 carbamidomethylation as a fixed modification, precursor mass tolerances of 20 ppm for the first
161 search and 4.5 ppm for the main search, and a maximum FDR of 1% for both peptides and
162 proteins.

163 **Cell culture**

164 *Oxytricha trifallax* cells were cultured in Petri dishes or large Pyrex dishes containing
165 Pringsheim medium (0.11 mM Na₂HPO₄, 0.08mM MgSO₄, 0.85 mM Ca(NO₃)₂, 0.35 mM KCl,
166 pH 7.0) and fed *Chlamydomonas reinhardtii* and *Klebsiella pneumoniae* according to previously
167 published methods (Khurana et al. 2014). Matings were performed by starving the compatible
168 parental mating types 310 and 510, mixing the mating types, and diluting to a concentration of
169 about 5,000 cells per milliliter in Pringsheim medium and plating the cells in 10 cm plastic Petri
170 dishes. Matings were assessed several hours after mixing mating types by calculating the
171 percentage of paired cells per total cells.

172 **Reverse transcription PCR (RT-PCR)**

173 Cell cultures or mating time-courses were concentrated by centrifugation and total RNA
174 was extracted using Trizol. Turbo DNase (Thermo Fisher, Waltham, MA, USA) was used to
175 digest DNA before extracting RNA again. Eluted DNA-free total RNA was reverse transcribed
176 using oligo (dT) and AMV reverse transcriptase (New England Biolabs, Ipswich, MA, USA).
177 PCR was performed using cDNA template and Phusion High Fidelity DNA polymerase (New
178 England Biolabs, Ipswich, MA, USA).

179 **Nanochromosome assembly**

180 Pooled F1 cells were sequenced using Illumina sequencing. Short reads were mapped to
181 the germline MIC genome. Reads mapping to g111288 were isolated. Next, we searched for the

182 5' and 3' end of an arbitrary read mapping to g111288 in the other reads. We iterated the process
183 of searching for the 5' or 3' end of each read in the remaining reads until we found a read
184 terminating with a telomere repeat (C₄A₄). We manually assembled the sequences of the reads
185 into an g111288 nanochromosome.

186 **In vitro transcription**

187 To prepare long single-stranded RNA (ssRNA) transcripts for microinjection, PCR
188 primers were first designed to use Phusion High-Fidelity DNA polymerase (New England
189 Biolabs, Ipswich, MA, USA) to amplify the coding sequence of the desired TGLO and add a T7
190 promoter to the gene. The T7-flanked product was cloned using the TOPO TA cloning kit
191 (Thermo Fisher, Waltham, MA, USA) and Sanger sequenced (Genewiz, South Plainfield, NJ,
192 USA) to verify the insert. In vitro transcription was done using the HiScribe T7 High Yield RNA
193 Synthesis Kit according to the manufacturer's instructions (New England Biolabs, Ipswich, MA,
194 USA).

195 **RNA injection**

196 In vitro transcribed RNA was extracted using Trizol and resuspended to a concentration
197 of 3 micrograms per microliter. ssRNA was microinjected into mating cells at 12 hours post-
198 mixing according to previously published protocols (Fang et al. 2012). Post-injected cells were
199 allowed to recover in Volvic water for two days before picking single cells and plating them in
200 Volvic to establish clonal lines.

201 **5' rapid amplification of cDNA ends (5' RACE)**

202 We used a published 5' RACE protocol (Scotto-Lavino et al. 2006) with minor changes.
203 Briefly, total RNA was extracted in Trizol (Thermo Fisher, Waltham, MA, USA) and treated

204 with Turbo DNase (Ambion). One microgram of DNase-treated total RNA was reverse
205 transcribed using AMV reverse transcriptase (New England Biolabs, Ipswich, MA, USA) and a
206 gene-specific primer for either the germline-limited gene or actin II control. cDNA was poly(A)
207 tailed using terminal transferase (New England Biolabs, Ipswich, MA, USA). The A-tailed
208 cDNA was amplified using two rounds of PCR amplification using Phusion High-Fidelity DNA
209 Polymerase (New England Biolabs, Ipswich, MA, USA). The first round of amplification was
210 done over 15 cycles, the first round product was diluted 1:1000, the diluted first round product
211 was amplified over 35 cycles, and the products from the second round of amplification were
212 resolved on an agarose gel and stained with ethidium bromide (Bio-Rad, Hercules, CA).

213 **RT-qPCR**

214 As we did previously, we reverse transcribed total RNA from two different times during
215 the organism's life cycle using random hexamer primers. This cDNA was used as template in a
216 series of RT-qPCR experiments to detect the expression of either germline-limited ORF
217 candidate or actin. We used Power Sybr Green qPCR Master Mix (Thermo Fisher, Waltham,
218 MA, USA) and custom qPCR primers (Integrated DNA Technologies, Coralville, IA, USA) and
219 performed the reaction using a CFX384 Touch Real-Time PCR Detection System (Bio-Rad,
220 Hercules, CA, USA). We analyzed the C_q values using a standard curve method and compared
221 the number of transcripts in each sample to the number of small subunit mitochondrial rRNA.

222 **Southern hybridization**

223 1 µg of genomic DNA was resolved on a 1% agarose gel, and ethidium bromide was used
224 for visualization. MAC DNA was purified according to previously published methods (Swart et
225 al. 2013). Dilute PCR products were used as a control to approximate the expected copy number
226 in the genomic DNA lanes. The 1 Kb Plus DNA ladder (Thermo Fisher, Waltham, MA, USA)
227 was used as a size standard. After gel electrophoresis, DNA was blotted onto a nylon membrane,
228 detected using a digoxigenin-labeled DNA probe, and detected using chemiluminescence
229 according to a previously published protocol (Yerlici et al. 2019)

230 **Primers**

231 The following primers were synthesized by Integrated DNA Technologies (Coralville, IA, USA)
232 for use in this study.

233 g104149 retention fwd: 5'-CGATGATGATGCAGAGCAGTGGAGGCTTAG-3'

234 g104149 retention rev: 5'-CATATCGTGTTCATTCATGTAAGATAACTACTGCTTG-3'

235 g67186 retention fwd: 5'-CAATTCACATAATCCTCTATTTCTGCAACTTTTTCTAGAC-3'

236 g67186 retention rev: 5'-

237 GAATTATTTGTAAATACTTGACTGACTCATTGTTGATAAAATGATTTAC-3'

238 QT RACE: 5'-CCAGTGAGCAGAGTGACGAGGACTCGAGCTCAAGC-3' (Scotto-Lavino
239 2006)

240 QO RACE: 5'-CCAGTGAGCAGAGTGACG-3' (Scotto-Lavino 2006)

241 QI RACE: 5'-GAGGACTCGAGCTCAAGC-3' (Scotto-Lavino 2006)

242 Actin II RT: 5'-GTGGTGAAGTTATATCCTCTCTTGCCAATAATG-3'

243 Actin II GSP 1: 5'-TGGCATGAGGAATTGCGTAACCTTCATAGA-3'

244 Actin II GSP 2: 5'-TCCATCTCCAGAGTCAAGCACAAACACC-3'

245 g104149 RT: 5'-TTGGGTAAATTCTGGCCAACCTCCCTTG-3'

246 g104149 GSP 1: 5'-CCAAGCTTCTCTGCACCTCATCCGTGAACA-3'

247 g104149 GSP 2: 5'-GTCTGCCCATCCACGATTTCACTGACC-3'

248 g67186 RT: 5'-AGCCTTGGTCCCTTCTGAGGCAG-3'

249 g67186 GSP 1: 5'-CCTGGCAAGAGCAACTTGACAGCAC-3'

250 g67186 GSP 2: 5'-GAGAGGCCAGAGGCTTCATTGCATACC-3'

251 g104149 gene qPCR fwd: 5'-CCAAGCTTCTCTGCACCTCATCCGTGAACA-3'

252 g104149 gene qPCR rev: 5'-AAGGTCAGTGAAATCGTGGATGGGCAGACT-3'

253 g67186 gene qPCR fwd: 5'-TGCAATGAAGCCTCTGGCCTCTCA-3'

254 g67186 gene qPCR rev: 5'-CCTGGCAAGAGCAACTTGACAGCAC-3'

255 g67186 upstream qPCR fwd: 5'-

256 CAATTCAATAGCACCGAATAGAAAGCTTATTTTATACAAGGATTAG-3'

257 g67186 upstream qPCR fwd: 5'-

258 CTAGATTTAATTA AAACTTGAAATGTCTACAGCCCATTAATAATTCG-3'

259 Actin II qPCR fwd: 5'-GGTGTGTGCTTGACTCTGGAGATGGA-3'

260 Actin II qPCR rev: 5'-TGGCATGAGGAATTGCGTAACCTTCATAGA-3'

261 Mitochondrial 23S rDNA qPCR fwd: 5'-GATAGGGACCGAACTGTCTCACG-3' (Nowacki et

262 al. 2009)

263 Mitochondrial 23S rDNA qPCR rev: 5'-CATATCCTGGTTGTGAATAATCTTCCAAGGG-3'

264 (Nowacki et al. 2009)

265 Telomere primer 1: 5'-

266 ACTATAGGGCACGCGTGGTCGACGGCCCGGGCTGGTCCCCAAAACCCCAAACCCC

267 AAAA -3' (Nowacki et al. 2008)

268 Telomere primer 2: 5'-ACTATAGGGCACGCGTGGT-3' (Nowacki et al. 2008)

269 g43073 TSP 1: 5'-GCCAGGTAGTTGCAAGCGCTCTCGAGAG-3'

270 g43073 TSP 2: 5'-GCTCAAAGTTTTAACTACTTGATTGAAGTGTAGATTTGGCAATC-3'

271 g104149 TSP 1: 5'-GTAAATTCTGGCCAACCTCCCTTGAGTTCCAAGCTTC-3'

272 g104149 TSP 2: 5'-CAAAGTCTGCCCATCCACGATTTCACTGACCTTTG-3'

273 g93797 TSP 1: 5'-GCCCAATTCATATGCTGCTTCTTTGAGCCACTTG-3'

274 g93797 TSP 2: 5'-GATCTGGTTTTACAGTTGAGGTAGTAGTAG-3'

275 g111288 fwd PCR: 5'-CTCTACTCTCTTAGGTCTCCCTCTGCCATT-3'

276 g111288 rev PCR: 5'-AGCGGCCTGAACTTTGTAAGGAGTAAGAT-3'

277 Actin II fwd PCR: 5'-GACTCAAATTATGTTTGAAGTCTTCAATGTACCTTGCC-3'

278 Actin II rev PCR: 5'-GTGGTGAAGTTATATCCTCTCTTGGCCAATAATG-3'

279 g111288 nanochromosome gene fwd qPCR: 5'-CAGGCCGCTTTAACTGCAACCATAGTTG-

280 3'

281 g111288 nanochromosome gene rev qPCR: 5'-

282 GGAAATTGAGCCAACCTTACAGTTAGAGCC-3'

283 g111288 nanochromosome MDS2 fwd qPCR: 5'-

284 CTTTCCTACAAATCCCCTTAAATTTCCAGTCTTGTAC-3'

285 g111288 nanochromosome MDS2 rev qPCR: 5'-

286 GTACCATGCTAGGATGTTATTGAAATCATAGAAGAC-3'

287 g111288 nanochromosome MDS4 fwd qPCR: 5'-

288 CGTCAAATTCAGTAACTAGCTCAGGTACGTC-3'

289 g111288 nanochromosome MDS4 rev qPCR: 5'-CTACCCTCCCGAGGAAAATACCTGG-3'

290 g111288 nanochromosome MDS7 fwd qPCR: 5'-

291 CTGAAATGGCTGTATCTATGGTTATTATAAAGAATTAGTG-3'

292 g111288 nanochromosome MDS7 rev qPCR: 5'-CAATCATCACTCTCCCTAACCGTACCTC-
293 3'

294 g111288 nanochromosome IES6 fwd qPCR: 5'-
295 GGGAAAGTTATTTTATTATGAGTTTAGGTTGCATTCATTC-3'

296 g111288 nanochromosome IES6 rev qPCR: 5'-
297 GAATGAAAATGAGTGAATTAAGAATTTTAATGAAGTATGATATAACATTC-3'

298 **Bioinformatic analyses**

299 Short read DNA sequences were locally aligned to reference sequences using Bowtie 2
300 (Langmead and Salzberg 2012) or BWA-MEM. Short read RNA sequences were aligned to
301 reference sequences using HISAT2 (Kim et al. 2019). Sanger sequencing DNA reads were
302 aligned to reference sequences using the Geneious aligner in the Geneious software package
303 (version 5.9) (Biomatters, Ltd., Auckland, New Zealand) with default parameters.

304 **Data availability**

305 All cell stocks are available upon request. Illumina sequencing datasets were uploaded to
306 the NCBI Short Read Archive under the BioProject PRJNA665991. The authors affirm that all
307 data necessary for confirming the conclusions of the article are present within the manuscript and
308 figures.

309 **Results**

310 **Thousands of transcribed germline-limited open reading frames (TGLOs) are expressed** 311 **during development.**

312 We examined potential germline-limited coding sequences in the *Oxytricha trifallax* MIC
313 genome by searching for transcribed germline-limited open reading frames, which we refer to as
314 TGLOs. We adapted a computational pipeline originally used to identify 810 germline-limited
315 protein coding genes expressed during *Oxytricha trifallax* development (Figure 1A, left) (Chen
316 et al. 2014). First, we used Augustus gene prediction (Stanke et al. 2006) and RNA sequencing
317 hints from throughout the organism's life cycle to predict 217,805 potential coding sequences in
318 the germline genome. To exclude potential coding sequences that are present in the somatic
319 MAC genome or are not transcribed at significant levels, we restrict TGLOs to computationally
320 predicted ORFs with virtually no DNA sequencing coverage in the MAC genome of both
321 parental strains. Another requirement is that they have RNA expression in at least one timepoint
322 during the organism's life cycle. To set read mapping thresholds appropriate for the variable
323 sequencing depth of individual RNA and DNA libraries, we used a Monte Carlo approach in
324 which the predicted 217,805 candidate loci were randomly shuffled 100 times throughout the
325 germline-limited portion of the MIC genome, while recording the distribution of the number of
326 DNA and RNA reads mapped to the random loci. The distributions of DNA or RNA reads
327 mapped to randomly shuffled TGLO loci were treated as the background germline-limited
328 coverage. We required that TGLOs have a number of DNA sequencing reads mapping to them
329 from either parent or the F1 progeny that is no greater than the fifth percentile from the
330 background germline-limited coverage simulation (i.e. no reads mapped per TGLO). On the
331 other hand, highly expressed TGLOs should have RNA sequencing coverage equal to at least the
332 95th percentile from the random distribution (i.e. four reads mapped per TGLO). We also used a

333 lower RNA sequencing threshold (i.e. a minimum of two reads mapped per TGLO) because at
334 least one experimentally confirmed TGLO was not present in the high transcription TGLO
335 dataset. CD-HIT (Fu et al. 2012) and RepeatMasker (Smit et al. 2013) were used to cluster
336 similar sequences and to remove sequences associated with repetitive elements. The final
337 mutually exclusive datasets contained 4342 and 6296 TGLOs with high and low transcription
338 levels, respectively (Figure 1A, center). Like the previously reported germline-limited gene
339 dataset, TGLOs tend to be intron-poor, with 8.8% and 6.4% of high and low transcription
340 TGLOs, respectively, containing introns compared to 64.9% of MAC encoded genes. These
341 datasets update our previous estimates and contain 279 (213 and 66, resp.) of the 810 germline-
342 limited genes predicted in Chen et al. (2014) (Figure 1A, right) (Chen et al. 2014), with some of
343 the reduction attributed to strain-specific differences described below.

344 The previous set of 810 germline-limited genes included functional predictions (Chen et
345 al. 2014). We investigated conserved domains and putative gene functions using the functional
346 annotation tool eggNOG mapper (version 2) (Huerta-Cepas et al. 2017). 111 high transcription
347 TGLOs and 245 low transcription TGLOs mapped to conserved eggNOG orthology clusters
348 (version 5.0) (Figure 1B) (Huerta-Cepas et al. 2019). 54 TGLOs with functional predictions were
349 previously-predicted germline-limited genes (42 and 12 in high and low transcription TGLOs,
350 respectively). Predicted functions and conserved domains included several potentially involved
351 in DNA rearrangement and epigenetic regulation, including MT-A70, miRNA methylation,
352 DNA helicase, PHD zinc finger, and high mobility group.

353 Protein expression of TGLOs could also suggest a function role for a subset of predicted
354 coding sequences. One quarter (26%) of the original 810 germline-limited genes had peptides
355 identified in a nuclear proteome extracted from mid-rearrangement cells at a single timepoint
356 (Chen et al. 2014), and we queried the new TGLO datasets against this previously published

357 peptide dataset. 144 high and 48 low transcription TGLOs (101 and 42 newly discovered,
358 respectively) were present in this limited 40 hour proteomic survey. Several peptides from the
359 developmental survey were also mapped to TGLOs with eggNOG functional predictions (Figure
360 1B, blue text).

361 The previously published set of germline-limited genes was limited to developmental
362 gene expression, with most germline-limited genes transcribed beginning 40 hours after mixing
363 of parental cells (Chen et al. 2014). We assessed the transcription profiles of TGLOs throughout
364 the organism's developmental life cycle using a deeply sequenced set of developmental RNA
365 sequencing libraries. Two partially overlapping triplicate RNA sequencing time-courses across
366 post-zygotic development showed that RNA expression from both high (Figure 1C) and low
367 transcription TGLOs also clustered toward the later stages of rearrangement. Conversely, a
368 random sample of one thousand somatic MAC-encoded genes had a diverse set of RNA
369 expression profiles during the same time-course, suggesting that TGLOs are enriched in
370 developmental expression.

371 **TGLO genes are eliminated after gene expression.**

372 By definition, TGLO DNA sequences are restricted to the germline MIC. Since the
373 germline genome is diploid, TGLOs are present at a copy number equal to twice the number of
374 micronuclei per cell. Since DNA copy number changes significantly throughout MAC
375 development (Spear and Lauth 1976), we studied DNA copy number changes and elimination of
376 TGLOs during development. A preliminary copy-number study indicated that most TGLOs are
377 eliminated by the end of the developmental life cycle, but the DNA copy number profiles of
378 TGLOs are heterogeneous, with some showing very little copy number variation throughout
379 development, leaving it unclear whether the loci are eliminated from the developing somatic
380 MAC by the end of the sexual life cycle (Figure 2A).

381 Since we previously reported that telomeres are permissive to transcription in *O. trifallax*,
382 unlike in other lineages (Beh et al. 2019), we amplified several TGLO loci via telomere
383 suppression PCR (Chang et al. 2004) to determine whether telomeres are added upstream of
384 these loci before DNA elimination. We found that three out of six sampled TGLOs—
385 representing both high and low transcription TGLOs—had telomeres added near the ORF during
386 mid to late development and before their elimination from the developing somatic MAC (Figure
387 2B), consistent with their transcriptional pattern.

388 **Strain-specific germline-limited ORFs**

389 Our studies uncovered one case of a germline-encoded ORF that was also present at a
390 low copy level in the somatic MAC of one parent. The protein coding locus, OXYTRIMIC_220
391 (“g111288”), was included in the previously reported set of 810 MIC-limited genes, but it does
392 not encode any conserved functional domains nor was it detected in a developmental mass
393 spectrometry survey (Chen et al. 2014). The initial Augustus gene prediction identified this ORF.
394 However, it was later excluded from the pipeline after incorporating new DNA sequencing
395 libraries from the parent strains and F1 progeny, which suggested that g111288 is present in the
396 somatic MAC of at least one parental strain.

397 We used PCR to amplify g111288 from parental genomic DNA to test whether the locus
398 is present in the somatic genome of either parent strain. We found that the coding sequence was
399 abundant in strain JRB510, which was not the reference strain used for genome sequencing
400 (Swart et al. 2013; Chen et al. 2014). In addition, we found that several cell lines derived from
401 either single F1 progeny or genetically manipulated F1 lines also contained g111288 at
402 detectable DNA copy levels (Figure 3A). In addition, the g111288 locus varied in DNA copy
403 level in individual F1 lines derived from different parental crosses.

404 Since g111288 appeared to be present in the MAC genome of only parental strain,
405 JRB510, and germline limited in the reference strain JRB310, we investigated the nature of the
406 putative g111288 somatic MAC nanochromosome. Next generation sequencing reads from a
407 pool of F1 progeny cells were mapped to the germline MIC genome. This allowed assembly of
408 an entire g111288 nanochromosome with telomeres at both ends and indicated that it derives
409 from seven MDSs with the g111288 open reading frame entirely contained within the first MDS
410 (Figure 3B). RNA sequencing from developmental time-points confirmed that g111288 is
411 transcribed from 40 to 60 hr after mixing of both parental strains (Figure 3C). In addition,
412 alignment of RNA-seq reads to the other six MDSs on the g111288 nanochromosome suggested
413 the possibility that the other six MDSs of the g111288 nanochromosome could have coding
414 potential. To assess the nanochromosome's relative copy number in different cell lines, we
415 performed qPCR to target different amplicons across the g111288 nanochromosome using
416 template genomic DNA from parental cells and F1 progeny lines. A two order of magnitude
417 copy number increase was consistently observed in the JRB510 parent line relative to the
418 reference JRB310 strain (Figure 3D). Moreover, three F1 lines displayed copy levels somewhat
419 higher than the JRB510 parental strain, and the other two F1 lines appeared to have few to no
420 copies of the nanochromosome, like strain JRB310. Southern hybridization with a probe
421 targeting a MAC-specific MDS-MDS junction region confirmed the presence of the
422 nanochromosome in MAC DNA from parental strain JRB510 as well as two F1 cell lines
423 (SLC89 and SLC92; Seegmiller et al. 1996) (Figure 3E).

424 Since g111288 is present in the somatic genome of several F1 lines and at a low level in
425 one parent, we assessed whether the coding sequence is transcribed during asexual (vegetative)
426 growth. However, we did not detect any transcripts from this locus outside the middle and late
427 stages of developmental, corresponding to approximately 48 hours after mixing of mating-

428 compatible cells (Figure 3F). Swart et al. (2013) previously reported that many other MAC
429 nanochromosomes have developmental-specific expression (Swart et al. 2013), suggesting that
430 g111288 is a strain-specific nanochromosome, retained only in the MAC genome of JRB510 and
431 passed on to its F1 progeny.

432 **Few ncRNAs map to TGLO loci**

433 *Oxytricha*'s genome rearrangements and DNA deletion are regulated by noncoding
434 RNAs (ncRNAs). For example, Otiwi-1-bound piRNAs map to retained MDSs but not germline-
435 limited regions or IESs (Fang et al. 2012), and long template RNAs map to nanochromosomes in
436 the MAC genome (Lindblad et al. 2017). Hence, we mapped template RNAs and Otiwi-1-
437 associated piRNAs to the MIC genome and assessed their coverage in TGLO loci and the
438 g111288 locus. We found that Otiwi-1 piRNAs map to MDSs more heavily than TGLOs (Figure
439 4A). Otiwi-1 piRNAs aligned to g111288, which is retained at a low somatic copy level in one
440 parent (Figure 4B), but piRNAs are present at a reduced level compared to neighboring MDSs.
441 Template RNA coverage was also significantly higher in MDSs compared to TGLOs (Figure
442 4C), although the strain-specific TGLO g111288 lacked any template RNAs despite being
443 encoded by the JRB510 MAC (Figure 4D).

444 **Synthetic RNA injection can protect TGLO loci from genomic deletion**

445 g111288 presents an example of a potential coding sequence that is present in the somatic
446 MAC of one strain while eliminated as a TGLO in another strain. We decided to test whether
447 exposure to artificial RNAs during development could reprogram the germline-limited status of
448 TGLOs, thereby retaining them on MAC nanochromosomes. Given our previous observations
449 that exposure to non-coding RNAs can reprogram IES retention in the MAC (Fang et al. 2012;
450 Khurana et al. 2018 RNA; Beh et al. 2019) we used RNA injection to test whether exposure to

451 targeting RNA could reprogram the retention of two TGLO loci during development (Figure
452 5A). We targeted two TGLO loci that are encoded in the IESs of other MAC loci. One of the two
453 candidates, g67186, was previously predicted to encode a histone 2B gene (Chen et al. 2014),
454 while the other, g104149, did not contain any predicted conserved domains. The two candidates
455 are also among the highest expressed TGLOs that mapped within IESs, facilitating our strategy
456 (Figure 5A). Importantly, we also observed that our candidate TGLOs lacked Otiwi-1 piRNAs
457 and template RNAs during the sexual life cycle (Figure 5B), suggesting that the cell does not
458 endogenously encode their somatic retention during the sexual life cycle.

459 PCR from cell cultures derived from single injected cells, followed by Sanger sequencing
460 indicated that RNA injection did reprogram IES+TGLO retention in some progeny, with varying
461 levels of retention based on differences in PCR band sizes. Some products contained small
462 deletions in the retained sequence relative to the reference MIC locus, but no deletions affected
463 the ORF (Figure 5C and 5D). No F1 lines from uninjected WT parental cells contained the
464 TGLO sequences, suggesting that RNA injection specifically programs the somatic DNA
465 retention (Figure 5E right and Figure 5F right).

466 RNA programmed IES retention was previously shown to be heritable after subsequent
467 sexual cycles, so we also tested whether the IES+TGLO insertions were retained after
468 backcrossing to a parental strain. PCR amplification from genomic DNA of backcrossed pools of
469 cells indicated that the retained TGLO g104149 was partially heritable for at least two more
470 generations (Figure 5E, left). The other retained TGLO, g67186, was partially heritable for one
471 backcrossed generation (Figure 5F, left). A second band corresponding to the wild-type product
472 was present in both backcrosses, consistent with the presence of WT nanochromosomes in the
473 backcrosses to the wild-type parental strain.

474 **Retained TGLOs are transcribed outside usual developmental program**

475 Our engineered strains that retain TGLO loci are unique in their ability to encode
476 previously eliminated germline sequences in their macronucleus. Genome-wide transcription
477 start site profiling in asexually growing *O. trifallax* cells showed that transcription initiation
478 typically occurs in the subtelomeric sequence of somatic nanochromosomes that encode a single
479 gene, and this is usually within approximately one hundred bases of the transcribed coding
480 sequence (Beh et al. 2019). Since the retained TGLO reading frames are nested within the
481 protein coding sequences of a flanking gene, but also retain their own putative upstream and
482 downstream regulatory sequences, we assessed the expression of retained TGLOs. We collected
483 total RNA from asexually growing cells with the retained TGLO, as well as WT parental lines,
484 and a WT developmental time-course when TGLOs are normally transcribed, and amplified
485 cDNA ends using 5' RACE (Figure 6A). We found that retained TGLO loci were now
486 transcribed during both the asexual life cycle as well as at their normal developmental pattern
487 (Figure 6B bottom and Figure 6C bottom). The size of the RACE products were similar for the
488 retained lines as well as during normal developmental expression, suggesting that the
489 endogenous TSS was used for gene expression

490 Given the structural differences between the somatic MAC nanochromosome in asexually
491 growing cells and the differentiating MAC during the sexual life cycle, the transcriptional
492 environment of the two nuclei could differ greatly. We used qRT-PCR to compare the
493 transcription levels of retained TGLO loci during the asexual life cycle vs. WT TGLO
494 expression during development, finding that the transcription level of retained TGLOs is
495 approximately an order of magnitude higher during the WT developmental timepoint compared
496 to artificial expression during the asexual life cycle in retained lines (Figures 6D and 6E).

497 **Discussion**

498 Here, we introduce the definition of TGLO as a transcribed germline-limited DNA
499 sequence with the ability to encode a putative protein. We show that the *O. trifallax* germline
500 MIC genome contains abundant TGLOs that are transcribed to varying degrees in WT cells
501 during development, and are then eliminated from the somatic MAC. This suggests that TGLO
502 gene expression may be regulated by DNA elimination. The conserved domains and predicted
503 functions found in TGLO datasets also support this hypothesis. Moreover, as ciliates have
504 heterochromatic MIC genomes that are not amenable to transcription (Gorovsky and Woodard
505 1969), and previous observations demonstrated that *Oxytricha*'s germline MIC lacks RNA
506 polymerase II expression (Khurana et al. 2014). Therefore, it is an attractive hypothesis that this
507 lineage may have evolved mechanisms of shutting down gene transcription by programmed
508 DNA elimination after activating gene expression during development.

509 The earlier report of 810 germline-limited genes in *O. trifallax* assumed that germline-
510 limited coding sequences would be deleted before the cell returned to the asexual life cycle
511 (Chen et al. 2014). Here we present evidence instead that the timing of DNA elimination of
512 TGLOs is heterogeneous during the sexual life cycle. Furthermore, we note the transient addition
513 of *de novo* telomeres in unexpected locations accompanying TGLO transcription, a step that
514 might activate them for transcription. Conceptually similar, in a related ciliate *Euplotes crassus*,
515 DNA processing during the sexual life cycle is responsible for modulating the transcription of
516 one of three telomerase catalytic subunit genes (Karamysheva et al. 2003). Finally, our DNA
517 sequencing results suggest that most TGLOs are indeed eliminated from the somatic MAC by the
518 end of the sexual life cycle. However, we cannot exclude the possibility that a subset of TGLOs
519 persist longer, as further research into later developmental time-points could reveal.

520 We also observed that at least one germline-encoded ORF, g111288, is actually present at
521 a low somatic copy level in one parental cell line. Unlike TGLOs, g111288 is variably retained
522 as a high copy nanochromosome in some F1 progeny. Presumably, the presence of ncRNAs
523 derived from one parent can program retention of the chromosome in F1 cells, but the
524 incomplete penetrance of somatic g111288 heritability correlates with its low somatic copy
525 number in the JRB510 cell line. Curiously, g111288 does not appear to be transcribed from the
526 somatic MAC in either the parent nor F1 progeny. This is unexpected because the entire coding
527 sequence is present on its own nanochromosome along with its putative upstream and downstream
528 regulatory sequences. However, it is possible that its gene expression requires other *trans*-acting
529 regulatory factors specific to the developmental life cycle.

530 The case of g111288 is also noteworthy because it appears capable of being either
531 germline-restricted or somatic-encoded. At the level of smaller MDS or IES regions, flexibility
532 between being retained vs. deleted has been observed before but on an evolutionary timescale
533 (Mollenbeck et al. 2006) rather than an intraspecies difference (Vitali et al. 2019). This feature
534 itself could contribute to the birth of new genes, since new coding sequences can sometimes arise
535 from retained noncoding sequences if transcribed and functional (Neme and Tautz 2016; Neme
536 et al. 2017). A previous study in *Tetrahymena* reported that a set of developmentally transcribed
537 somatic minichromosomes are gradually eliminated from the MAC after genome rearrangement
538 (Lin et al. 2016). Moreover, a specific minichromosome in one *Tetrahymena* species might be
539 germline-limited in another species. This *Tetrahymena* example and our functional experiments
540 that reprogram somatic TGLO retention in *O. trifallax* suggest that TGLOs might be a reservoir
541 of sequences with somatic coding potential. We can envision an evolutionary model by which
542 germline-encoded sequences can gain access to the somatic genome where they would be

543 expressed. A deeper intraspecies survey of MAC and MIC genomes, together with
544 developmental RNAseq to survey expression, would be needed to test this hypothesis.

545 Our ability to program the somatic retention of specific TGLOs via ncRNA injection is a
546 unique feature of the present study. This had the ability to unmask gene expression of targeted
547 TGLOs outside their normal developmental program. *Tetrahymena thermophila* also has non-
548 maintained chromosomes that are lost soon after expression during development and can be
549 fused to adjacent regions to program their retention in the somatic MAC (Feng et al. 2017). Here
550 we have extended this general phenomenon to *Oxytricha* and showed that somatic retention
551 subverts the cell's endogenous transcription of the gene locus. This supports the hypothesis that
552 TGLO elimination represses their gene expression. In our example the misexpression of a single
553 TGLO locus did not affect cell viability, but the ensemble of loci may need to be silenced during
554 asexual growth.

555 .

556 **Acknowledgements**

557 The authors thank Virginia A. Zakian, Gertrud M. Schüpbach, Samuel Sternberg, and the
558 current and past members of the Landweber lab for their helpful feedback throughout the study.
559 We are grateful to Xiao Chen for bioinformatic help with selecting TGLO candidates. We would
560 also like to thank Wei Wang and Jessica Buckles at the Princeton University Genomics Core
561 Facility for their high-throughput sequencing expertise. This work was funded by NIH
562 R35GM122555 and NSF DMS1764366 to LFL.

563 **References**

- 564 Allen, S. E., Hug, I., Pabian, S., Rzeszutek, I., Hoehener, C., and Nowacki, M. (2017). Circular
565 concatemers of ultra-short DNA segments produce regulatory RNAs. *168*: 990-999.
- 566 Allen, S. E. and Nowacki, M. (2020). Roles of noncoding RNAs in ciliate genome architecture.
567 *J. Mol. Biol.* S0022-2836: 30026-30027.
- 568 Beh, L. Y., Debelouchina, G. T., Clay, D. M., Thompson, R. E., Lindblad, K. A., Hutton, E. R.,
569 Bracht, J. R., Sebra, R. P., Muir, T. W., and Landweber, L. F. (2019). Identification of a
570 DNA N6-adenine methyltransferase complex and its impact on chromatin organization.
571 *Cell* 177: 1781-1796.
- 572 Bryant, S. A., Herdy, J. R., Amemiya, C. T., and Smith, J. J. (2016). Characterization of
573 somatically-eliminated genes during development of the sea lamprey (*Petromyzon*
574 *marinus*). *Mol. Biol. and Evol.* 33: 2337-2344.
- 575 Burns, J., Kukushkin, D., Lindblad, K., Chen, X., Jonoska, N., and Landweber, L. F. (2016). : a
576 database of ciliate genome rearrangements. *Nucleic Acids Res.* 44: D703-D709.
- 577 Chang, W. J., Stover, N. A., Addis, V. M., and Landweber, L. F. (2004). A micronuclear locus
578 containing three protein-coding genes remains linked during macronuclear development
579 in the spirotrichous ciliate *Holosticha*. *Protist*, 155: 245-255.
- 580 Chen, X., Bracht, J. R., Goldman, A. D., Dolzhenko, E., Clay, D. M., Swart, E. C., Perlman, D.
581 H., Doak, T. G., Stuart, A., Amemiya, C. T., Sebra, R. P., and Landweber, L. F. (2014).
582 The architecture of a scrambled genome reveals massive levels of genomic
583 rearrangement during development. *Cell* 158: 1187-1198.

- 584 Clay, D. M., Yerlici, V. T., Villano, D. J., and Landweber, L. F. (2019). Programmed
585 Chromosome Deletion in the Ciliate *Oxytricha trifallax*. *G3* 9: 3105-3118.
- 586 Curtis, E. A. and Landweber, L. F. (2006). Evolution of gene scrambling in ciliate micronuclear
587 genes. *Ann. N. Y. Acad. Sci.* 870: 349-350.
- 588 Fang, W., Wang, X., Bracht, J. R., Nowacki, M., and Landweber, L. F. (2012). Piwi-interacting
589 RNAs protect DNA against loss during *Oxytricha* genome rearrangement. *Cell* 151:
590 1243–1255.
- 591 Feng, L., Wang, G., Hamilton, E. P., Xiong, J., Yan, G., Chen, K., Chen, X., Dui, W., Plemens,
592 A., Khadr, L., et al. (2017). A germline-limited piggyBac transposase gene is required for
593 precise excision in *Tetrahymena* genome rearrangement. *Nucleic Acids Res.* 45: 9481–
594 9502.
- 595 Fu, L., Niu, B., Zhu, Z., Wu, S., and Li, W. (2012). CD-HIT: accelerated for clustering the next-
596 generation sequencing data. *Bioinformatics*, 28: 3150-3152.
- 597 Gorovsky, M. A. and Woodard, J. (1969). Studies on nuclear structure and function in
598 *Tetrahymena pyriformis*: I. RNA synthesis in macro- and micronuclei. *The Journal of cell*
599 *biology*, 42: 673-682.
- 600 Hamilton, E. P., Kapusta, A., Huvos, P. E., Bidwell, S. L., Zafar, N., Tang, H., Hadjithomas, M.,
601 Krishnakumar, V., Badger, J. H., Caler, E. V., et al. (2016). Structure of the germline
602 genome of *Tetrahymena thermophila* and relationship to the massively rearranged
603 somatic genome. *eLife* 5: e19090.
- 604 Huerta-Cepas, J., Forslund, K., Coelho, L. P., Szklarczyk, D., Jensen, L. J., von Mering, C., and
605 Bork, P. (2017). Fast genome-wide functional annotation through orthology assignment
606 by eggNOG-mapper. *Mol. Biol. Evol.* 34: 2115–2122.

- 607 Huerta-Cepas, J., Szklarczyk, D., Heller, D., Hernández-Plaza, A., Forslund, S. K., Cook, H.,
608 Mende, D. R., Letunic, I., Rattei, T., Jensen, L. J., et al. (2019). eggNOG 5.0: a
609 hierarchical, functionally and phylogenetically annotated orthology resource based on
610 5090 organisms and 2502 viruses. *Nucleic Acids Res.* 47: D309–D314.
- 611 Itoh, Y., Kampf, K., Pigozzi, M. I., and Arnold, A. P. (2009). Molecular cloning and
612 characterization of the germline-restricted chromosome sequence in the zebra finch.
613 *Chromosoma* 118: 527-536.
- 614 Karamysheva, Z., Wang, L., Shrode, T., Bednenko, J., Hurley, L. A., and Shippen, D. E. (2003).
615 Developmentally programmed gene elimination in *Euplotes crassus* facilitates a switch in
616 the telomerase catalytic subunit. *Cell*, 113: 565-576.
- 617 Khurana, J. S., Clay, D. M., Moreira, S., Wang, X., and Landweber, L. F. (2018). Small RNA-
618 mediated regulation of DNA dosage in the ciliate *Oxytricha*. *RNA* 24: 18-29.
- 619 Khurana, J. S., Wang, X., Chen, X, Perlman, D. H., and Landweber, L. F. (2014). Transcription-
620 independent functions of an RNA polymerase II subunit, Rpb2, during genome
621 rearrangement in the ciliate, *Oxytricha trifallax*. *Genetics* 197: 839-849.
- 622 Kim, D., Paggi, J. M., Park, C., Bennett, C., and Salzberg, S. L. (2019). Graph-based genome
623 alignment and genotyping with HISAT2 and HISAT-genotype. *Nat. Biotechnol.* 37: 907–
624 915.
- 625 Kinsella, C. M., Ruiz-Ruano, F. J., Dion-Côté, A. M., Charles, A. J., Gossmann, T. I., Cabrero,
626 J., Kappei, D., Hemmings, N., Simons, M. J. P., Camacho, J. P. M., et al. (2019).
627 Programmed DNA elimination of germline development genes in songbirds. *Nat.*
628 *Commun.* 10: 5468.

- 629 Langmead, B. and Salzberg, S. L. (2012). Fast gapped-read alignment with Bowtie 2. Nat.
630 Methods 9: 357-359.
- 631 Li, H., Handsaker, B., Wysoker, A., Fennell, T., Ruan, J., Homer, N., Marth, G., Abecasis, G.,
632 Durbin, R., and 1000 Genome Project Data Processing Subgroup. (2009). The sequence
633 alignment/map format and SAMtools. Bioinformatics, 25: 2078-2079.
- 634 Liao, Y., Smyth, G. K., and Shi, W. (2014). featureCounts: an efficient general purpose program
635 for assigning sequence reads to genomic features. Bioinformatics, 30: 923-930.
- 636 Lin, C. G., Lin, I. T., and Yao, M. C. (2016). Programmed minichromosome elimination as a
637 mechanism for somatic genome reduction in *Tetrahymena thermophila*. PLoS Genet. 12:
638 e1006403.
- 639 Lindblad, K. A., Bracht, J. R., Williams, A. E., and Landweber, L. F. (2017). Thousands of
640 RNA-cached copies of whole chromosomes are present in the ciliate *Oxytricha* during
641 development. RNA 23: 1200-1208.
- 642 Lindblad, K. A., Pathmanathan, J. S., Moreira, S., Bracht, J. R., Sebra, R. P., Hutton, E. R., and
643 Landweber, L. F. (2019). Capture of complete ciliate chromosomes in single sequencing
644 reads reveals widespread chromosome isoforms. BMC Genom. 20: 1037.
- 645 Love, M. I., Huber, W., and Anders, S. (2014). Moderated estimation of fold change and
646 dispersion for RNA-seq data with DESeq2. Genome Biol. 15: 550.
- 647 Meyer, G. F. and Lipps, H. J. (1981). The formation of polytene chromosomes during
648 macronuclear development of the hypotrichous ciliate *Stylonychia mytilus*. Chromosoma,
649 82: 309-314.

- 650 Möllenbeck, M., Cavalcanti, A. R., Jönsson, F., Lipps, H. J., and Landweber, L. F. (2006).
651 Interconversion of germline-limited and somatic DNA in a scrambled gene. *J. Mol. Evol.*,
652 63: 69-73.
- 653 Neme, R., Amador, C., Yildirim, B., McConnell, E., and Tautz D. (2017). Random sequences are
654 an abundant source of bioactive RNAs or peptides. *Nat. Ecol. Evol.* 1: 0217.
- 655 Neme, R. and Tautz, D. (2016). Fast turnover of genome transcription across evolutionary time
656 exposes entire non-coding DNA to de novo gene emergence. *eLife* 5: e09977.
- 657 Nowacki, M., Higgins, B. P., Maquilan, G. M., Swart, E. C., Doak, T. G., and Landweber, L. F.
658 (2009). A functional role for transposases in a large eukaryotic genome. *Science* 324:
659 925-928.
- 660 Nowacki, M., Vijayan, V., Zhou, Y., Schotanus, K., Doak, T. G., and Landweber, L. F. (2008).
661 RNA-mediated epigenetic programming of a genome-rearrangement pathway. *Nature*
662 451: 153–158.
- 663 Pigozzi, M. I. and Solari, A. J. (1998). Germ cell restriction and regular transmission of an
664 accessory chromosome that mimics a sex body in the zebra finch, *Taeniopygia guttata*.
665 *Chromosome Res.* 6: 105-113.
- 666 Pigozzi, M. I. and Solari, A. J. (2005). The germ-line-restricted chromosome in the zebra finch:
667 recombination in females and elimination in males. *Chromosoma* 114: 403-409.
- 668 Prescott, D. M. (1994). The DNA of ciliated protozoa. *Microbiol. Rev.* 58: 233–267.
- 669 Scotto-Lavino, E., Du, G., and Frohman, M. A. (2006). 5' end cDNA amplification using classic
670 RACE. *Nat. Protoc.* 1: 2555-2562.

- 671 Seegmiller, A., Williams, K. R., Hammersmith, R. L., Doak, T. G., Witherspoon, D., Messick,
672 T., Storjohann, L. L., and Herrick, G. (1996). Internal eliminated sequences interrupting
673 the *Oxytricha* 81 locus: allelic divergence, conservation, conversions, and possible
674 transposon origins. *Mol. Biol. Evol.* 13: 1351-1362.
- 675 Smit, A. F. A., Hubley, R., and Green, P. RepeatMasker Open-4.0. (2013)
676 <<http://www.repeatmasker.org>>.
- 677 Smith, J. J., Antonacci, F., Eichler, E. E., and Amemiya, C. T. (2009). Programmed loss of
678 millions of base pairs from a vertebrate genome. *Proc. Natl. Acad. Sci. U.S.A.* 106:
679 11212-11217.
- 680 Smith, J. J., Baker, C., Eichler, E. E., and Amemiya, C. T. (2012). Genetic consequences of
681 programmed genome rearrangement. *Curr. Biol.* 22: 1524–1529.
- 682 Spear, B. B. and Lauth, M. R. (1976). Polytene chromosomes of *Oxytricha*: biochemical and
683 morphological changes during macronuclear development in a ciliated protozoan.
684 *Chromosoma* 54: 1-13.
- 685 Stanke, M., Keller, O., Gunduz, I., Hayes, A., Waack, S., and Morgenstern, B. (2006).
686 AUGUSTUS: ab initio prediction of alternative transcripts. *Nucleic Acids Res.* 34:
687 W435-W439.
- 688 Swart, E. C., Bracht, J. R., Magrini, V., Minx, P., Chen, X., Zhou, Y., Khurana, J. S., Goldman,
689 A. D., Nowacki, M., Schotanus, K., et al. (2013). The *Oxytricha trifallax* macronuclear
690 genome: a complex eukaryotic genome with 16,000 tiny chromosomes. *PLoS Biol.* 11:
691 e1001473.

- 692 Timoshevskiy, V. A., Herdy, J. R., Keinath, M. C., and Smith, J. J. (2016). Cellular and
693 molecular features of developmentally programmed genome rearrangement in a
694 vertebrate (sea lamprey: *Petromyzon marinus*). PLoS Genet. 12: e1006103.
- 695 Timoshevskiy, V. A., Lampman, R. T., Hess, J. E., Porter, L. L., Smith, J. J. (2017). Deep
696 ancestry of programmed genome rearrangement in lampreys. Dev. Biol. 429: 31-34.
- 697 Torgasheva, A. A., Malinovskaya, L. P., Zadesenets, K. S., Karamysheva, T. V., Kizilova, E. A.,
698 Akberdina, E. A., Pristyazhnyuk, I. E., Shnaider, E. P., Volodkina, V. A., Saifitdinova, A.
699 F. et al. (2019). Germline-restricted chromosome (GRC) is widespread among songbirds.
700 Proc. Natl. Acad. Sci. U.S.A. 116: 11845-11850.
- 701 Vitali, V., Hagen, R., and Catania, F. (2019). Environmentally induced plasticity of programmed
702 DNA elimination boosts somatic variability in *Paramecium tetraurelia*. Genome Res.,
703 29: 1693-1704.
- 704 Wang, J., Gao, S., Mostovoy, Y., Kang, Y., Zagoskin, M., Sun, Y., Zhang, B., White, L. K.,
705 Easton, A., Nutman, T. B. et al. (2017). Comparative genome analysis of programmed
706 DNA elimination in nematodes. Genome Res. 27: 2001-2014.
- 707 Wang, J., Mitreva, M., Berriman, M., Thorne, A., Magrini, V., Koutsovoulos, G., Kumar, S.,
708 Blaxter, M. L., and Davis, R. E. (2012). Silencing of germline-expressed genes by DNA
709 elimination in somatic cells. Dev. Cell 23: 1072–1080.
- 710 Yerlici, V. T., Lu, M. W., Hoge, C. R., Miller, R. V., Neme, R., Khurana, J. S., Bracht, J. R., and
711 Landweber, L. F. (2019). Programmed genome rearrangements in Oxytricha produce
712 transcriptionally active extrachromosomal circular DNA. Nucleic Acids Res. 47: 9741–
713 9760.

714 **Figure legends**

715 **Figure 1: Germline-limited ORFs are expressed during *Oxytricha trifallax* genome**
716 **rearrangement.**

717 (A) Left: Pipeline for predicting TGLOs in *Oxytricha trifallax* germline MIC genome. Center:
718 Total number of computationally predicted candidates remaining after each pipeline step. Right:
719 Total number of MIC-limited genes (Chen et al. 2014) remaining after each pipeline step. (B)
720 EggNOG mapper-predicted functions and conserved domains in TGLOs. Blue text indicates that
721 peptides from the associated TGLOs were present in a single nuclear proteome surveyed during
722 rearrangement (Chen et al. 2014). (C) Log₂-normalized RNA-seq read counts of High and Low
723 transcription TGLOs and one thousand randomly selected somatic MAC-encoded genes across
724 the *Oxytricha trifallax* developmental life cycle (hours labeled post mixing of compatible mating
725 types). Color scale refers to the log₂-normalized RNA expression.

726 **Figure 2: TGLOs are eliminated from the developing MAC.**

727 (A) Log₂-normalized DNA copy number of High and Low transcription TGLOs across the
728 *Oxytricha trifallax* developmental life cycle. Color scale refers to the log₂-normalized DNA copy
729 number. (B) Telomere suppression PCR targeting the upstream telomere addition site of selected
730 TGLOs in genomic DNA samples collected throughout the *Oxytricha trifallax* developmental
731 life cycle.

732 **Figure 3: Parental cells can carry a strain-specific germline-limited ORF.**

733 (A) Top: PCR targeting g111288 or Actin II using genomic DNA from F1 lines, parent lines, and
734 other mutant F1 lines used in this study. Bottom: Genome track showing the approximate
735 location of g111288 PCR primers. Yellow: g111288, light blue: flanking MDSs. (B) The

736 germline genome locus containing g111288 with mapped F1 reads from a pool of asexually
737 growing F1 cells. Yellow: g111288, light blue: MDSs, dark blue: assembled g111288 MDSs
738 from pooled F1 reads, gray triangles: observed telomere addition sites. **(C)** The germline genome
739 locus (bottom) containing g111288 (yellow) and strain-specific MDSs (dark blue) with mapped
740 RNA-seq coverage (black) from several time-points during asexual growth (starved or encysted
741 cells) and hours post mixing of mating types during the sexual life cycle. **(D)** Top: Copy number
742 relative to mitochondrial rDNA based on qPCR targeting several amplicons on the g111288
743 nanochromosome, an IES within the corresponding germline locus, and two unrelated somatic
744 loci. Bottom: The germline genome locus containing g111288 with qPCR primer locations
745 indicated. Yellow: g111288, light blue: MDSs, dark blue: assembled g111288 MDSs from
746 pooled F1 reads, black arrows: qPCR primers. **(E)** Top: Southern blot of parental and F1 MAC
747 DNA detected using an MDS-MDS junction spanning DNA probe. Bottom: MIC genome track
748 showing the portions of MDSs 1 and 2 detected. **(F)** Top: RT-PCR targeting g111288 or Actin II
749 using RNA from the same cell lines as in (A). Bottom: Genome track showing the approximate
750 location of g111288 RT-PCR primers. Yellow: g111288, light blue: MDSs.

751 **Figure 4: TGLO loci have few Otiwi-1 piRNAs and template RNAs.**

752 **(A)** Distribution of normalized mapping quality-filtered Otiwi-1 piRNA read counts (Fang et al.
753 2012) mapped to High and Low transcription TGLOs compared to MDSs. Read counts were
754 normalized to reads per kilobase million (RPKM). Brackets and asterisks indicate statistically
755 significant differences between distributions. Statistical significance was assessed using the non-
756 parametric Kolmogorov–Smirnov (KS) test, and $P < 0.05$ was considered statistically significant.
757 **(B)** The germline genome locus containing the strain-specific TGLO g111288 (yellow), MDSs
758 (blue), and mapped Otiwi-1-associated piRNA coverage (gray) from several time-points during
759 rearrangement. **(C)** Distribution of normalized mapping quality-filtered template RNA read

760 counts (Lindblad et al. 2017) mapped to High and Low transcription TGLOs compared to MDSs.
761 Read counts were normalized to RPKM. Brackets and asterisks indicate statistically significant
762 differences between distributions. Statistical significance was assessed using the non-parametric
763 KS test, and $P < 0.05$ was considered statistically significant. **(D)** The germline genome locus
764 containing the strain-specific TGLO g111288 (yellow), MDSs (blue), and mapped template
765 RNA coverage (gray) from several time-points during rearrangement.

766 **Figure 5: RNA injection programs heritable TGLO retention.**

767 **(A)** Synthetic RNA injection scheme to program the retention of a TGLO (yellow) in an IES
768 between two MDSs (blue). Possible products can include telomere-capped (black)
769 nanochromosomes with the entire IES plus TGLO flanked by the MDSs of the wild-type
770 flanking locus. **(B)** The germline genome loci containing the programmed retention candidate
771 TGLOs g104149 and g67186 (yellow), MDSs (blue), and mapped piRNA or template RNA
772 coverage (gray) from several time-points during rearrangement. **(C)** Top: Cell culture PCR
773 targeting the IES containing g104149 from cell lines derived from single RNA injected mating
774 pairs. Middle: The expected retention product containing g104149 with PCR primer locations.
775 Yellow: g104149, light blue: MDSs, black arrows: PCR primers. Bottom: Sanger sequencing
776 chromatograms from PCR reactions in (B) aligned to the expected retention product containing
777 g104149 (yellow). **(D)** Top: Cell culture PCR targeting the IES containing the predicted histone
778 2B TGLO g67186 from cell lines derived from single RNA injected mating pairs. Middle: The
779 expected retention product containing g67186 with PCR primer locations. Yellow: g67186, light
780 blue: MDSs, black arrows: PCR primers. Bottom: Sanger sequencing chromatograms from PCR
781 reactions aligned to the expected retention product containing g67186 (yellow). **(E)** Top: PCR
782 targeting the IES containing g104149 using genomic DNA from parental cells, F1 retention cells,
783 F1 retention cells backcrossed to parental cells, and unmanipulated F1 lines. Bottom: The

784 expected retention product containing g104149 with PCR primers. Yellow: g104149, light blue:
785 MDSs, black arrows: PCR primers. **(F)** Top: PCR targeting the IES containing the predicted
786 histone 2B TGLO g67186 using genomic DNA from parental cells, F1 retention cells, F1
787 retention cells backcrossed to parental cells, and unmanipulated F1 lines. Bottom: The expected
788 retention product containing g67186 with PCR primers. Yellow: g67186, light blue: MDSs,
789 black arrows: PCR primers.

790 **Figure 6: Retained TGLOs are misexpressed during asexual life cycle.**

791 **(A)** Possible transcription start sites (black arrows) on a hypothetical rearranged somatic
792 nanochromosome after RNA injection to retain TGLOs (yellow). Green: target transcript
793 deriving from TGLO's putative upstream regulatory sequence. **(B)** Germline genome locus
794 containing g104149 (yellow) and gene-specific 5' RACE primers used to amplify transcription
795 start site. **(C)** 5' RACE products targeting the g104149 or Actin II transcription start site in RNA
796 from F1 retention cells, parental cells, and mid-rearrangement mated cells. TdT: terminal
797 transferase. **(D)** Germline genome locus containing g67186 (yellow) and gene-specific 5' RACE
798 primers used to amplify transcription start sites. **(E)** 5' RACE products targeting the g67186 or
799 Actin II transcription start site in RNA from F1 retention cells, parental cells, and mid-
800 rearrangement mated cells. TdT: terminal transferase. **(F)** g104149 or Actin II RNA transcript
801 levels based on qRT-PCR relative to mitochondrial rRNA. Error bars: standard deviation of three
802 biological replicates. **(G)** g67186 or Actin II RNA transcript levels based on qRT-PCR relative
803 to mitochondrial rRNA. Error bars: standard deviation of three biological replicates.

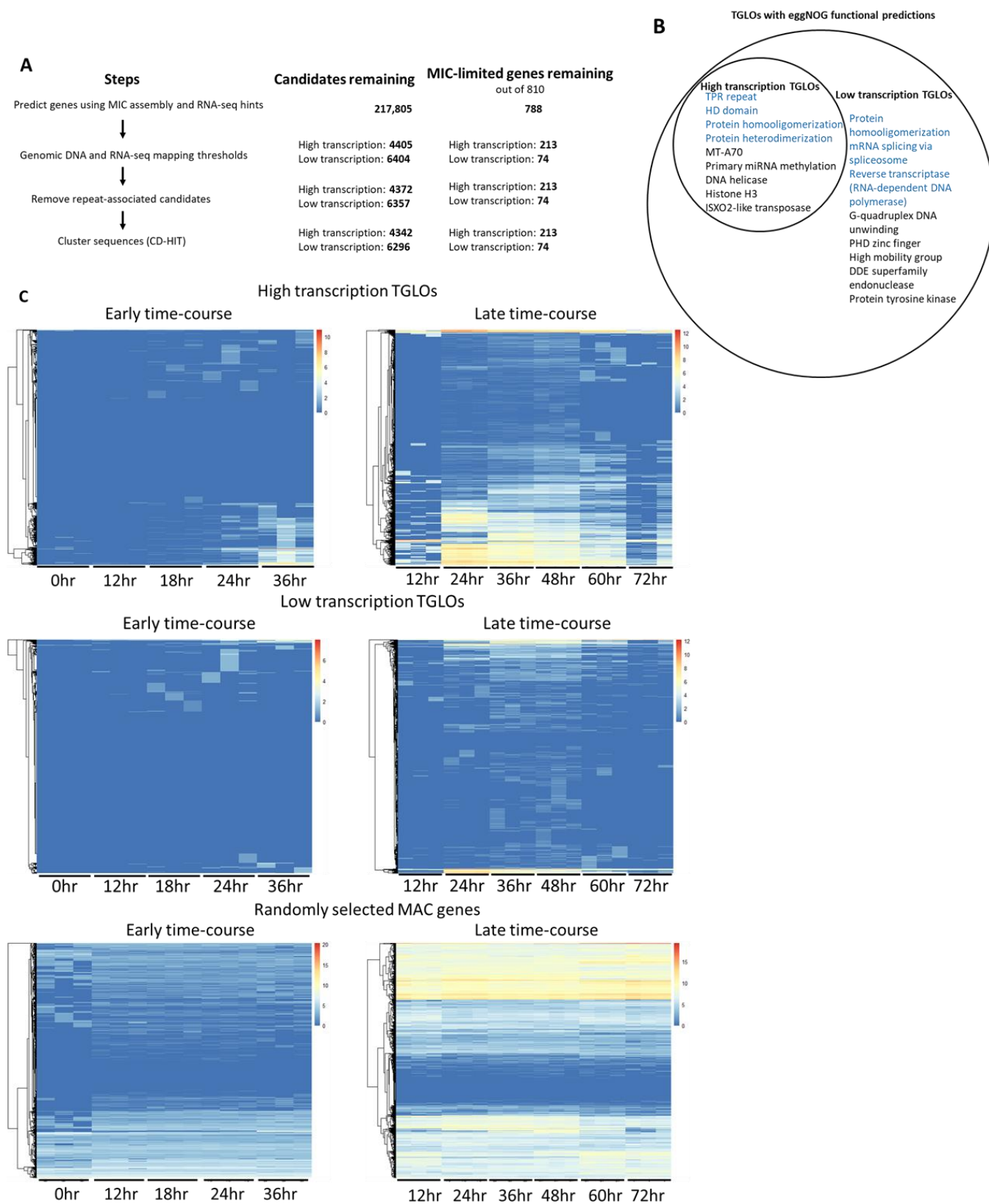


Figure 1

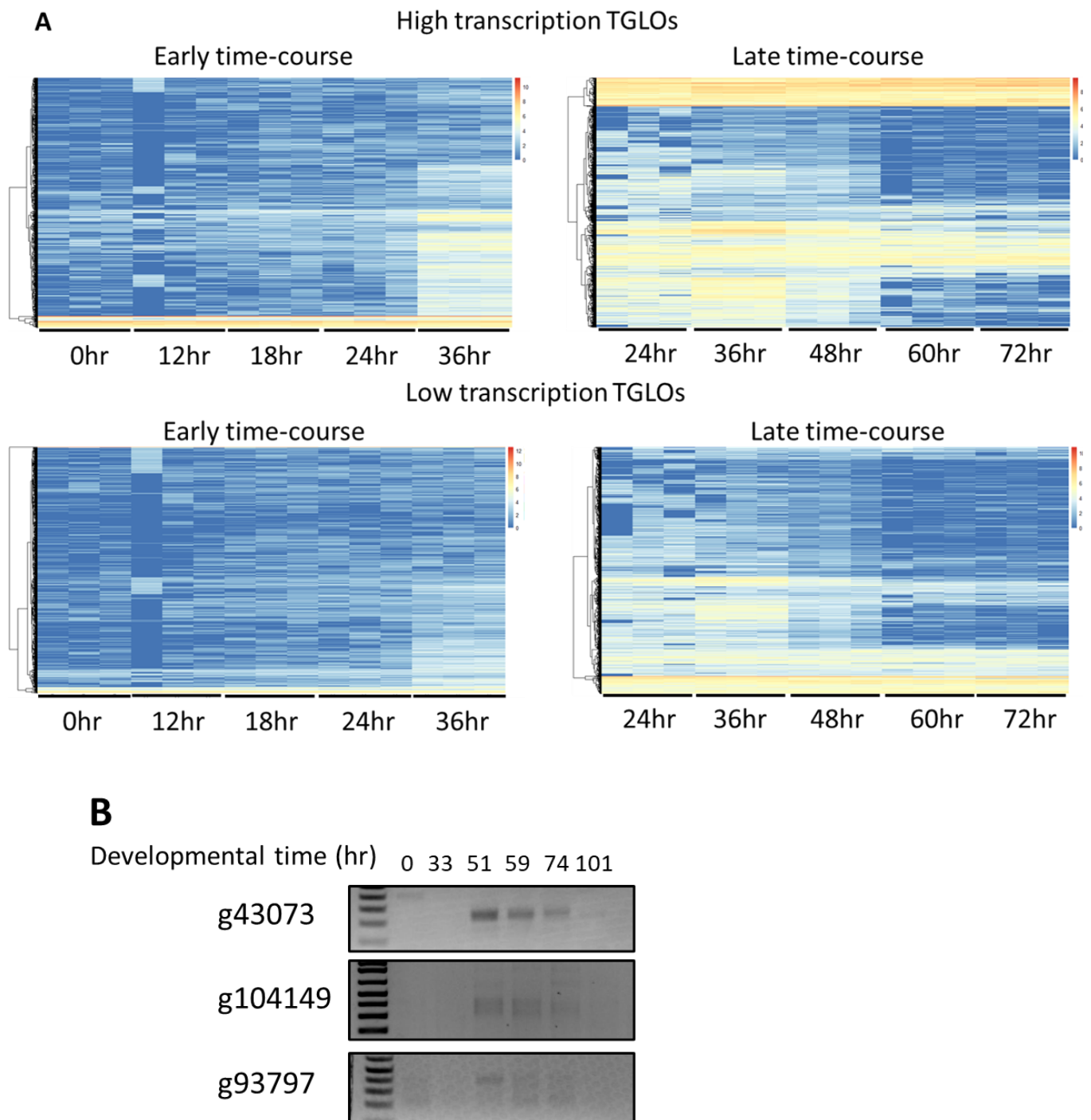


Figure 2

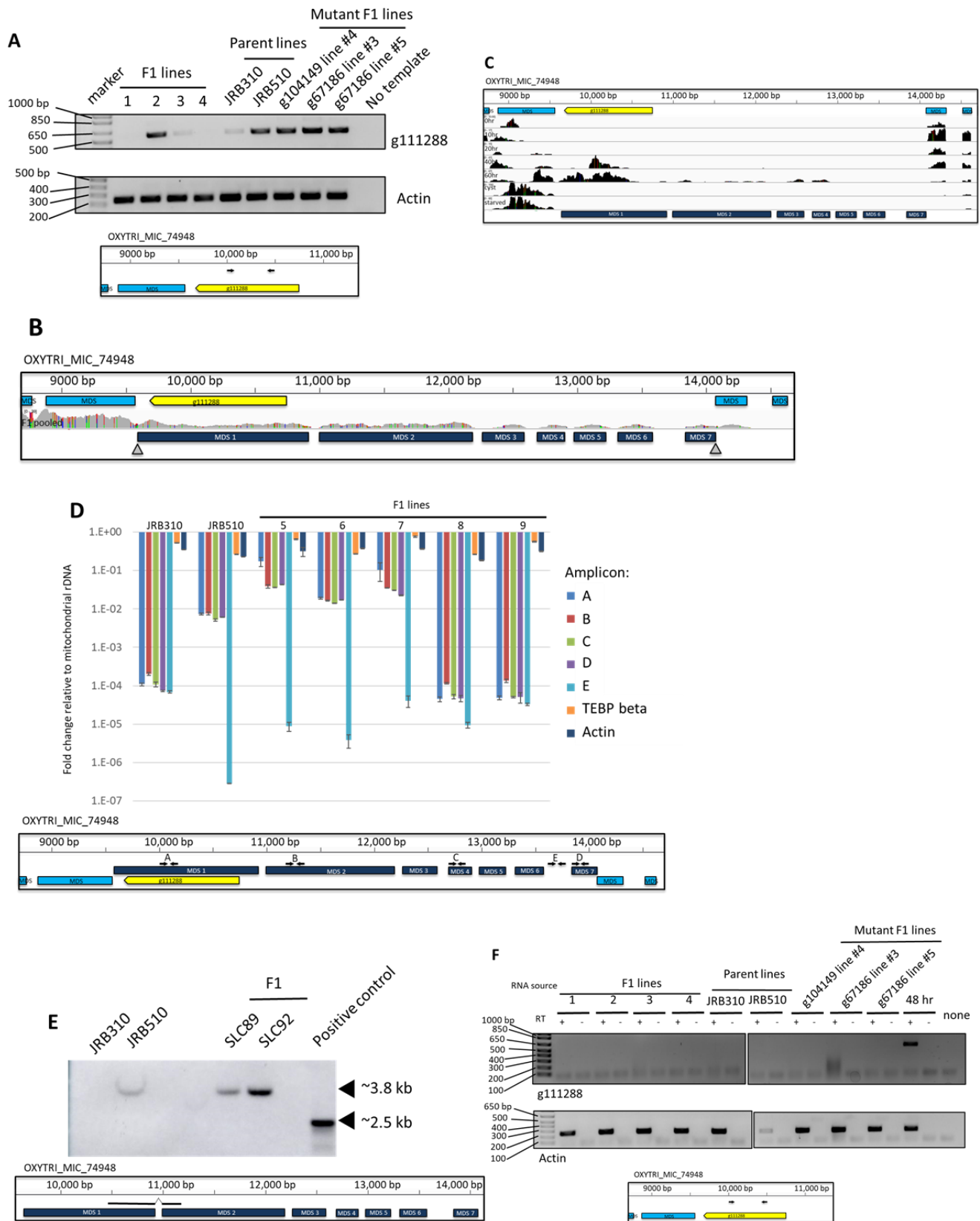


Figure 3

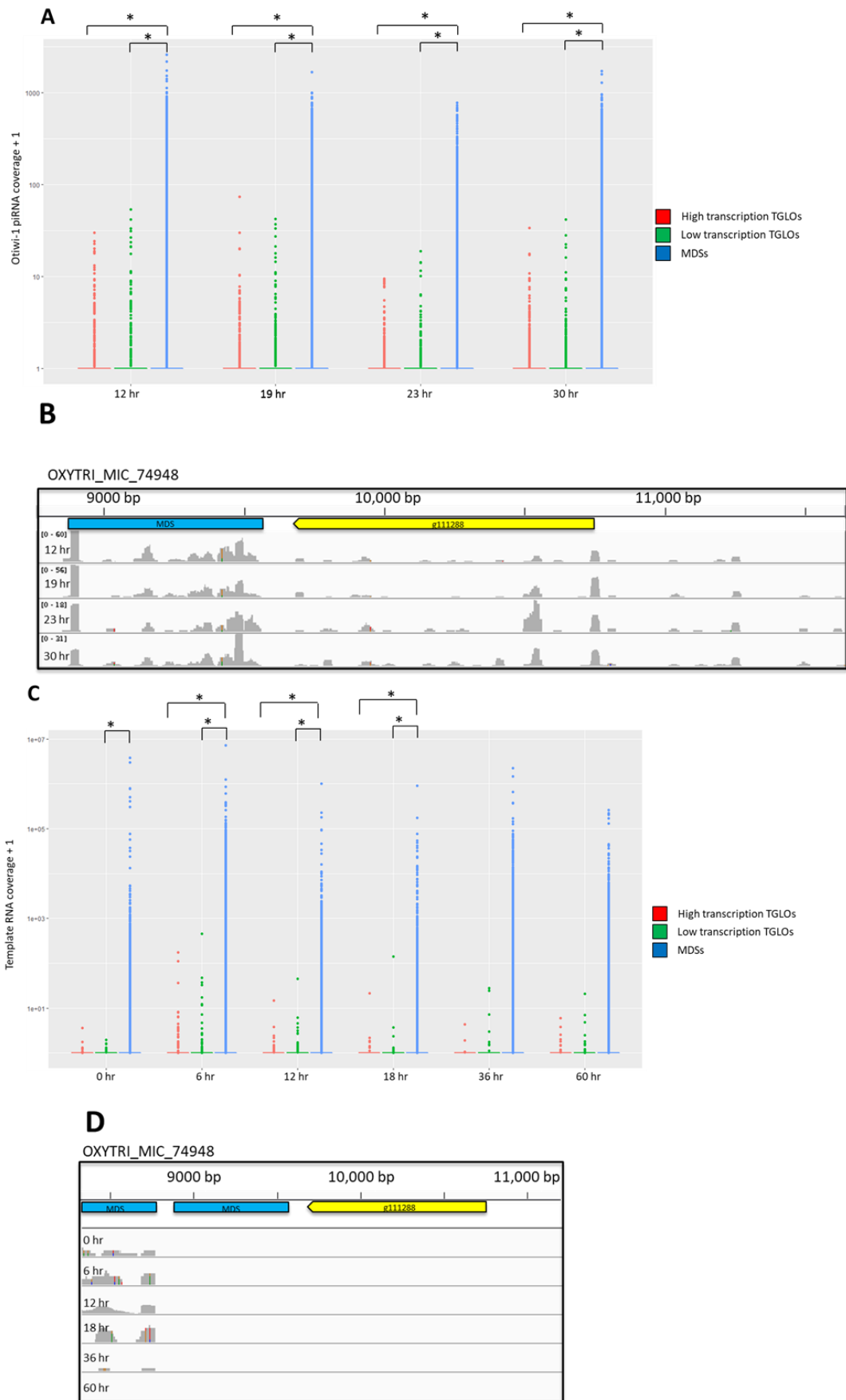


Figure 4

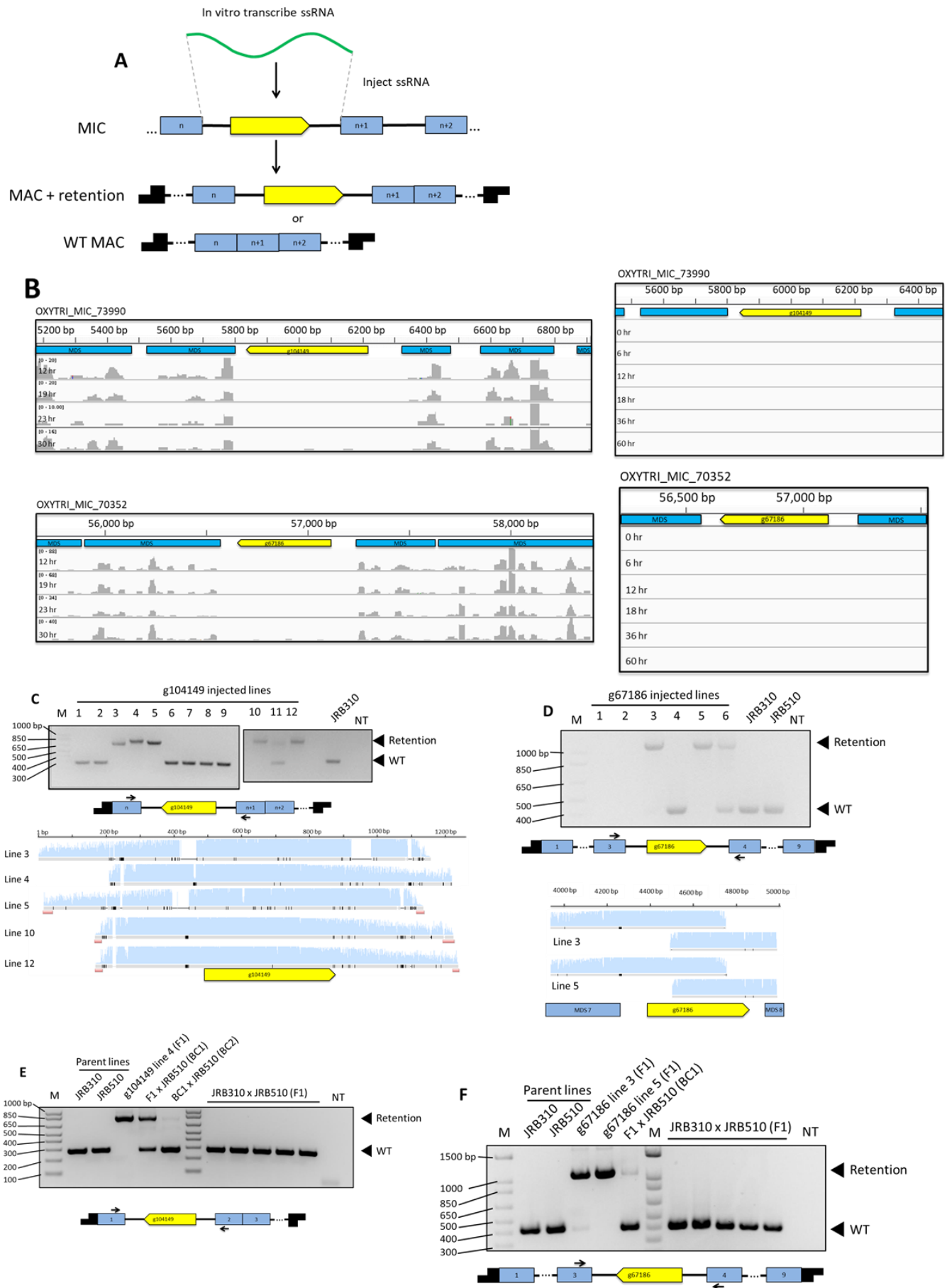


Figure 5

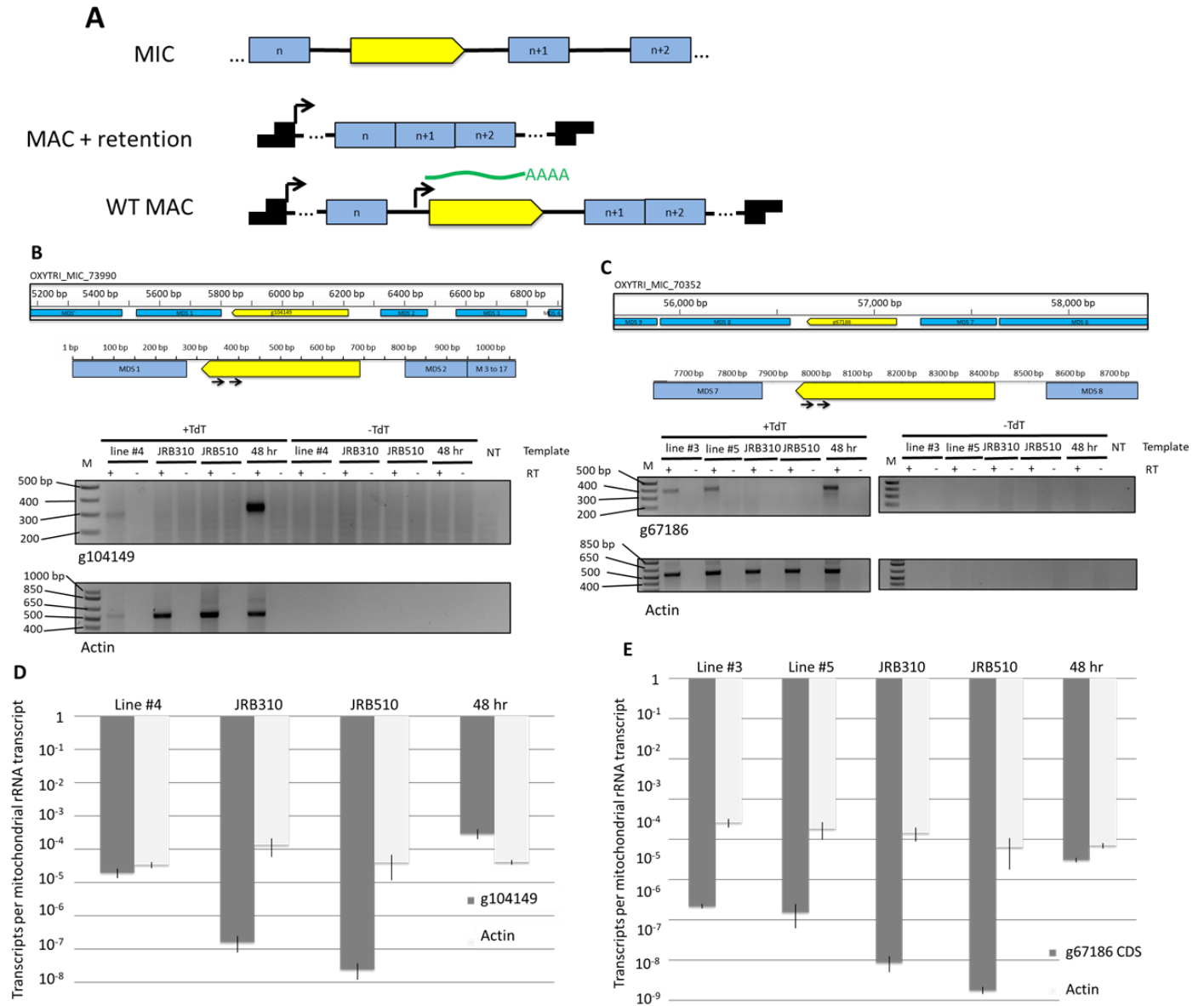


Figure 6